



HAL
open science

EFFECTS OF SLAB ROLLBACK ACCELERATION ON AEGEAN EXTENSION

Jean-Pierre Brun, Claudio Università Faccenna, Frederic Gueydan, Dimitrios Sokoutis, Melody Philippon, Konstantinos Kydonakis, Christian Gorini

► **To cite this version:**

Jean-Pierre Brun, Claudio Università Faccenna, Frederic Gueydan, Dimitrios Sokoutis, Melody Philippon, et al.. EFFECTS OF SLAB ROLLBACK ACCELERATION ON AEGEAN EXTENSION. Bulletin of the Geological Society of Greece, 2017, 50 (1), pp.5-23. 10.12681/bgsg.11697 . insu-01574659

HAL Id: insu-01574659

<https://insu.hal.science/insu-01574659>

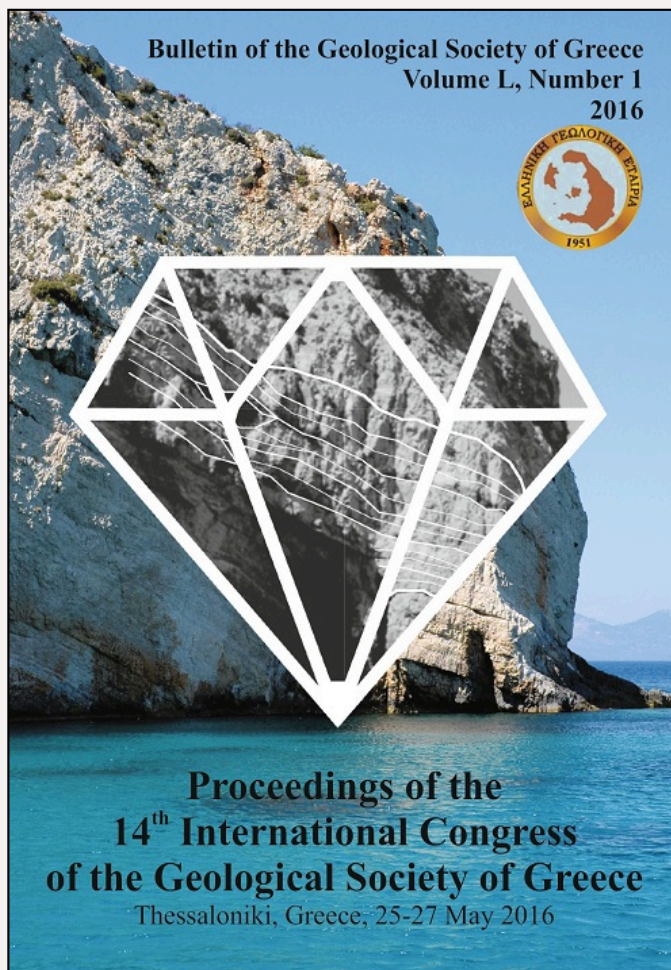
Submitted on 16 Aug 2017

HAL is a multi-disciplinary open access archive for the deposit and dissemination of scientific research documents, whether they are published or not. The documents may come from teaching and research institutions in France or abroad, or from public or private research centers.

L'archive ouverte pluridisciplinaire **HAL**, est destinée au dépôt et à la diffusion de documents scientifiques de niveau recherche, publiés ou non, émanant des établissements d'enseignement et de recherche français ou étrangers, des laboratoires publics ou privés.

Bulletin of the Geological Society of Greece

Vol. 50, 2016



EFFECTS OF SLAB ROLLBACK ACCELERATION ON AEGEAN EXTENSION

- | | |
|---------------------------|---|
| Brun J.-P. | Université Rennes 1,
Géosciences Rennes |
| Faccenna C. | LET, Laboratory of
Experimental Tectonics,
Università Roma Tre |
| Gueydan F.
Sokoutis D. | Department of Earth
Sciences, Faculty of
Geosciences, Utrecht
University |
| Philippon M. | Université des Antilles,
Géosciences Montpellier |
| Kydonakis K. | Université Rennes 1,
Géosciences Rennes |
| Gorini C. | Sorbonne Universités |
- <http://dx.doi.org/10.12681/bgsg.11697>

Copyright © 2016 J.-P. Brun, C. Faccenna, F. Gueydan, D. Sokoutis, M. Philippon, K. Kydonakis, C. Gorini



To cite this article:

Brun, Faccenna, Gueydan, Sokoutis, Philippon, . . . , & Gorini (2016). EFFECTS OF SLAB ROLLBACK ACCELERATION ON AEGEAN EXTENSION. Bulletin of the Geological Society of Greece, 50, 5-14.

EFFECTS OF SLAB ROLLBACK ACCELERATION ON AEGEAN EXTENSION

**Brun J.-P.¹, Faccenna C.², Gueydan F.³, Sokoutis D.^{4,5}, Philippon M.⁶,
Kydonakis K.¹ and Gorini C.⁷**

¹Université Rennes 1, Géosciences Rennes, UMR 6118 CNRS, bat. 15 - Campus de Beaulieu, 263 Av
du général Leclerc, BP 74205, 35042, Rennes Cedex, France, jean-pierre.brun@univ-rennes1.fr,
konstantinos.kydonakis@outlook.com

²LET, Laboratory of Experimental Tectonics, Università Roma Tre, Rome, Italy,
claudio.faccenna@uniroma3.it

³Université de Montpellier 2. Géosciences Montpellier, UMR5243, Université de Montpellier, Rue
Eugène Bataillon, France, frederic.gueydan@univ-montp2.fr

⁴Department of Earth Sciences, Faculty of Geosciences, Utrecht University, Budapestlaan 4, PO
Box 80021, 3508 Utrecht, The Netherlands, D.Sokoutis@uu.nl

⁵Department of Geosciences, University of Oslo, PO Box 1047, Blindern, N-0316 Oslo, Norway,
D.Sokoutis@uu.nl

⁶Université des Antilles, Géosciences Montpellier, UMR 5243, Campus de Fouillole, 97159,
Pointe à Pitre, France, Melodie.Philippon@gm.univ-montp2.fr

⁷Sorbonne Universités, UPMC Univ Paris 06, UMR 7193, ISTeP, F-75005, Paris, France,
christian.gorini@upmc.fr

Abstract

Aegean extension is a process driven by slab rollback that, since 45 Ma, shows a two-stage evolution. From Middle Eocene to Middle Miocene it is accommodated by localized deformation leading to i) the exhumation of high-pressure metamorphic rocks from mantle to crustal depths, ii) the exhumation of high-temperature rocks in core complexes and iii) the deposition of Paleogene sedimentary basins. Since Middle Miocene, extension is distributed over the whole Aegean domain giving a widespread development of onshore and offshore Neogene sedimentary basins. We reconstructed this two-stage evolution in 3D at Aegean scale by using available ages of metamorphic and sedimentary processes, geometry and kinematics of ductile deformation, paleomagnetic data and available tomographic models. The restoration model shows that the rate of trench retreat was around 0.6 cm/y during the first 30 My and then accelerated up to 3.2 cm/y during the last 15 My. The sharp transition observed in the mode of extension, localized versus distributed, which occurred in Middle Miocene correlates with the acceleration of trench retreat and is more likely a consequence of the Hellenic slab tearing documented by mantle tomography. The development of large dextral NE-SW strike-slip faults during the second stage of Aegean extension, since Middle Miocene, is illustrated by the 450 Km-long fault, recently put in evidence, offshore from Myrthes to Ikaria and onshore from Izmir to Balıkesir, in western Anatolia. Therefore, the interaction between the Hellenic trench retreat and the westward displacement of Anatolia started in Middle Miocene,

almost 10 Ma before the propagation of the North Anatolian Fault in the North Aegean. This raises a fundamental issue concerning the dynamic relationship between slab tearing and Anatolia displacement.

Keywords: Blueschists, core-complexes, basins.

1. Introduction

The Aegean Tertiary tectonic history, from a dynamic point of view, corresponds to back-arc extension driven by slab rollback (Royden, 1993; Jolivet and Faccenna, 2000; Faccenna *et al.*, 2003, 2014; Brun and Faccenna, 2008). Extension started around 45 Ma ago (Brun and Sokoutis, 2010) and accommodated up to 600 km of trench retreat (Jolivet and Brun, 2010; Jolivet *et al.*, 2013). Extension followed the closure of the two oceanic domains of Vardar and Pindos in Cretaceous-Eocene (Dercourt *et al.*, 1993; Channell and Kozur, 1997; Robertson, 2004) leading to the stacking of three continental blocks that from top to base are: Rhodopia, Pelagonia and Adria (Fig. 1).

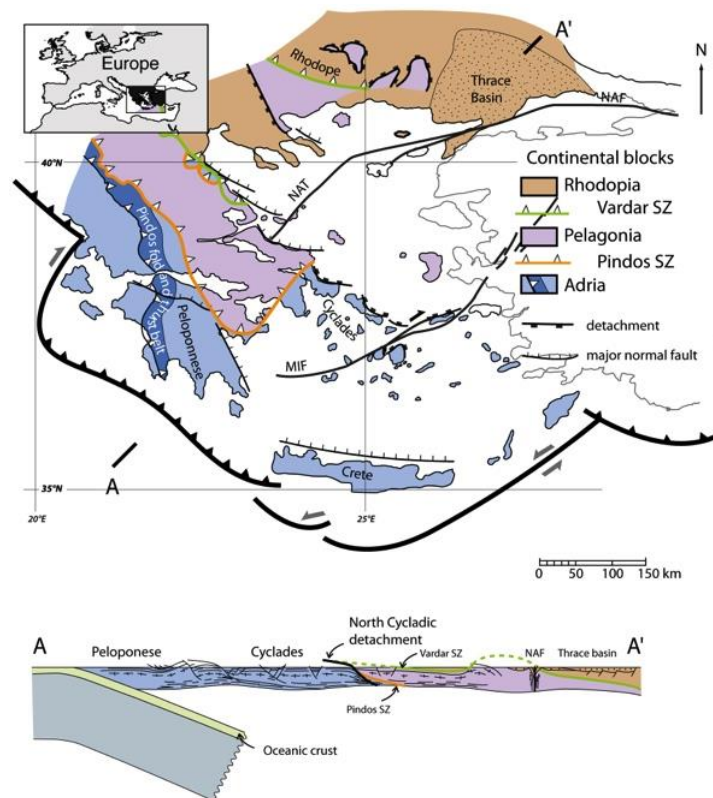


Figure 1 - The three main continental blocks of Aegean: Rhodopia, Pelagonia and Adria.

Tomographic models of the underlying mantle image a single slab (e.g. Wortel and Spakman, 2000; Piromallo and Morelli, 2003; Widiyantoro *et al.*, 2004) indicating that the convergence of continental blocks, now separated by two suture zones, has been accommodated by a single subduction. During subduction rollback, the Pelagonia and Adria crust panels were fully detached

from the downgoing lithospheric mantle and moved back to surface, resting directly on top of asthenosphere (Brun and Faccenna, 2008; Tirel *et al.*, 2013).

In the present study we show that Aegean extension occurred in two main stages, from Middle Eocene to Middle Miocene and since Middle Miocene. The significant large-scale features that characterized these two stages of extension are defined in terms of sedimentation, deformation and metamorphism. It is argued i) that the major dynamic change that occurred in Middle Miocene, resulted from an acceleration of trench retreat that is more probably responsible for the observed transition between localized and distributed modes of extension and ii) that the likely cause of this acceleration due to slab tearing coeval with the onset of Anatolia westward displacement.

2. The two main stages of Aegean extension

The first plate kinematic models of eastern Mediterranean (McKenzie, 1972, 1978; Le Pichon and Angelier, 1981) and the present-day displacement field from satellite geodesy (McClusky *et al.*, 2000; Hollenstein *et al.*, 2008; Müller *et al.*, 2013) show that the active Aegean extension results from the combined effects of the southwestward retreat of the Hellenic trench and the westward displacement of Anatolia along the North Anatolian Fault (NAF).

The geological record shows that this interaction between two strongly oblique components of boundary displacement started in Middle Miocene (Dewey and Şengör, 1979; Şengör *et al.*, 2005; Philippon *et al.*, 2014), around 10 My before the NAF reached the Aegean (Armijo *et al.*, 1999; Hubert-Ferrari *et al.*, 2003; Şengör *et al.*, 2005). On the other hand, the coeval extensional exhumation of high-pressure metamorphic rocks in the Southern Hellenides and high-temperature metamorphic rocks in the Rhodope (Brun and Sokoutis, 2007; Brun and Faccenna, 2008) started in Middle Eocene (see review of data in Jolivet and Brun, 2010 and Philippon *et al.*, 2012). This brief summary of the Aegean extension history during a large part of the Tertiary indicates a process that has not been continuous, neither in time nor in space. This is illustrated by a striking difference in the distribution of Paleogene and Neogene sedimentary basins at Aegean scale (Fig. 2) suggesting that a major change in the dynamics of Aegean extension occurred in Middle Miocene, more 30 My after its onset.

2.1. Stage 1: Paleogene basins and ductile exhumation of metamorphic rocks

Paleogene basins (Fig. 2a) that mostly contain Middle Eocene and/or Oligocene sediments are located i) on top of the Rhodopia block (Trace Basin: Görür and Okay, 1996; Siyako and Huvaz, 2007; Kiliyas *et al.*, 2013); Vardar-Thermaikos Basin: Roussos, 1994; Carras and Georgala, 1998) and ii) on top of Pelagonia (Mesohellenic Trough: Doutsos *et al.*, 1994; Ferrière *et al.*, 2004) (Fig. 2a).

The exhumation of core complexes (high-temperature metamorphism) and blueschists (high-pressure metamorphism) (Figs. 3 and 4) resulted from significantly different mechanisms of development, primarily controlled by temperature-dependent rheology of the crustal units.

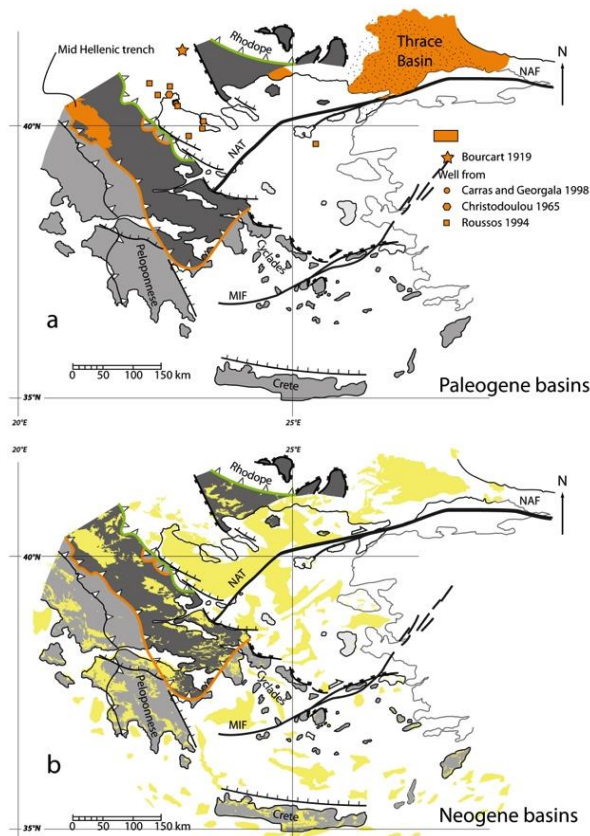


Figure 2 - Distribution of Paleogene (a) and Neogene (b) basins in the Aegean domain.

The location of core complexes and high pressure belts in the Aegean, as well as their relative timing of exhumation, has important dynamic implications:

- The Southern Rhodope Core Complex (SRCC) (Brun and Sokoutis, 2007) started to develop in Middle-Late Eocene in North Aegean when the Cycladic Blueschist Unit (CBU) started to exhume in central Aegean (Jolivet and Brun, 2010; Philippon *et al.*, 2012).
- The Central Cyclades Core Complex (CCCC) (Philippon *et al.*, 2012) developed in central Aegean almost synchronous with the exhumation onset of HP-LT Phyllite–Quartzite Nappe (PQN) in Peloponnese and Crete (Jolivet *et al.*, 2010).
- The sense of shear and detachment dip, in core complexes, and sense of shear, in high-pressure rocks, is top to SW in North Aegean (SRCC) (Brun and Sokoutis, 2007), to NE in central Aegean (CBU and CCCC) (Philippon *et al.*, 2012) and to E and N in South Aegean (HP-LT PQN) (Jolivet *et al.*, 2010).
- The part of exhumation synchronous with ductile deformation ended in Middle Miocene in all types of metamorphic rocks, either high-temperature (SRCC and CCCC) or high pressure (CBU and HP-LT PQN) and whatever age of onset.

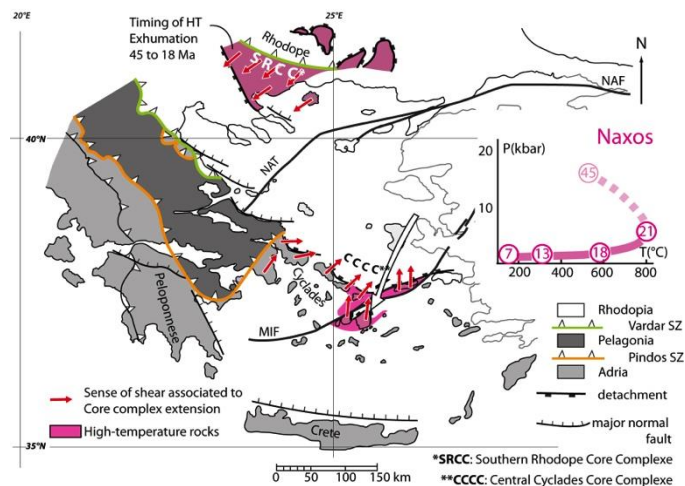


Figure 3 - The two core complexes (HT metamorphism) of the Aegean domain with corresponding PT diagrams and related senses of shear.

2.2. Stage 2: Neogene basins and dextral transtensional faulting

The Neogene basins (Fig. 2b) whose deposition started in Middle Miocene constitute one of the most striking geological features of the Aegean domain, both onshore and offshore. They emplaced on all types of rock units (Paleogene basins, high-temperature or high-pressure metamorphic units, plutonic massives and volcanic buildups) of Rhodopia, Pelagonia and Adria and over around 1000 km from Crete to Rhodope. The earlier deposits are Langhian-Serravalian in some basins but Tortonian sediments are present in most of them. Where structural data are available, field measurements or seismics, tectonic setting of most basins is extensional or transtensional (e.g. Mercier *et al.*, 1987, 1989; Lyberis, 1984; Mascle and Martin, 1990; Koukouvelas and Aydin, 2002; Sakellariou *et al.*, 2013).

Low-temperature thermochronology ages, obtained by various methods (apatite and zircon fission-track and U-Th/He on apatite and zircon) in high-temperature and high-pressure metamorphic units, which were exhumed during the first stage of extension, are dominantly Serravalian-Tortonian, over the whole Aegean (Brix *et al.*, 2002; Wuthrich, 2009; Philippon *et al.*, 2012; Marsellos *et al.*, 2014). This indicates that metamorphic rocks of the SRCC, the CBU-CCCC and Peloponnese-Crete, whose onsets of exhumation were different, were reaching the surface in Middle-Late Miocene.

The mode of extension during this second stage of Aegean extension is in strong contrast with the one that characterizes the first stage. Extension passed in Middle Miocene from the core complex mode to the wide rift mode (Buck, 1991; Brun, 1999), as demonstrated by the deposition of extensional or transtensional Neogene basins across the whole Aegean, offshore as well as onshore. The interruption of ductile exhumation in Middle Miocene, in all types of metamorphic rocks (HT as well as HP) whatever their age of onset, as well as the segmentation of the metamorphic units and the deposition of Neogene basins on top of them suggest that the transition between the two modes of extension was not progressive and likely occurred in a rather short delay.

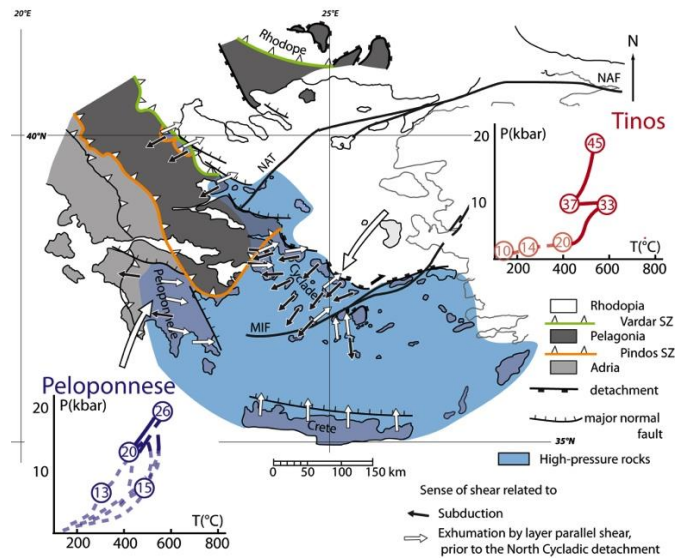


Figure 3 - The HP metamorphic domain of Adria and Pelagonia blocks with corresponding PTt diagrams and related senses of shear.

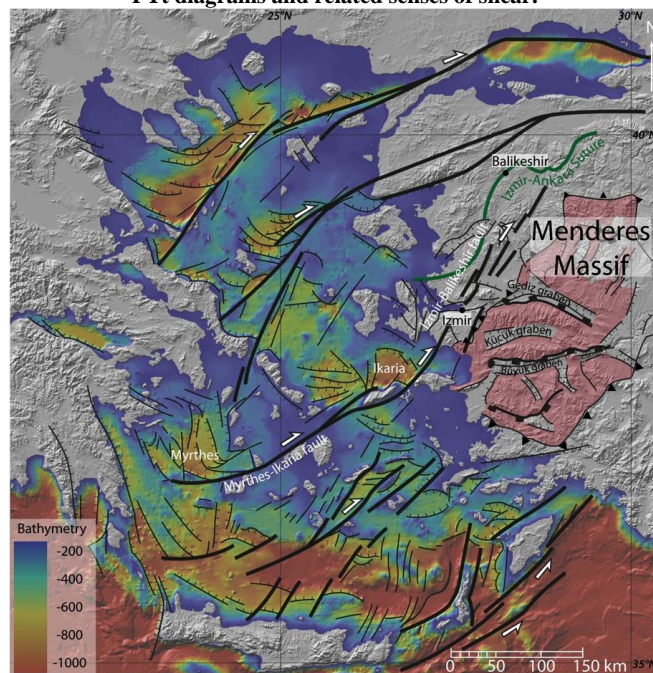


Fig. 4 - Major strike-slip faults and Neogene sedimentary basins in the Aegean Sea, as displayed by Aegean Sea bathymetry.

The Myrthes-Ikaria fault (MIF) (Philippon *et al.*, 2012) that cut through the whole Cyclades domain is the offshore extend of the onshore Ismir-Balikeshir transfer zone (IBTZ) (Sozobilir *et al.*, 2010; Ersoy *et al.*, 2012; Uzel *et al.*, 2013) (Fig. 4). Lower (?)–Late Miocene sedimentary–volcanic basins were deposited in this transtensional corridor, located at the northwestern border of the Menderes Massif (Ersoy *et al.*, 2012). Simultaneously, grabens developed in the Menderes, accommodating a NE–SW direction of stretching. Over 450 km, from Myrthes Basin to Balikeshir, this dextral strike-slip fault zone was active since Middle Miocene –i.e. around 10 My before the arrival of the NAT in the North Aegean. Whereas there is no direct evidence to identify when displacements ceased on this fault zone, it can be hypothesized that this occurred around 5 Ma when the NAF fully localized (Şengör *et al.*, 2005), in agreement with the youngest ages of exhumation recorded by low-temperature thermochronology in the Cyclades (Philippon *et al.*, 2014).

3. Discussion–Conclusion: Acceleration of slab rollback

The restoration of displacements using the numerous data sets available (paleomagnetism, kinematic indicators and geochronology) (Brun and Sokoutis, 2010 and re-evaluation by Brun *et al.*, 2012) shows that *an acceleration of trench retreat started in Middle Miocene* (Fig.5). The rate of trench retreat that was rather low, around 0.6 cm.y^{-1} , during the first stage of extension increased to around 1.7 cm.y^{-1} between Middle Miocene and Pliocene, reaching 3.2 cm.y^{-1} during the last 5 Ma. This acceleration of trench retreat (i.e. extensional boundary displacement), first by a factor 2 after Middle Miocene and then by a factor 5 after Pliocene, was more likely responsible for the observed change in the mode of extension, from localized to distributed - i.e. from core complex to wide rift (Buck, 1991; Brun, 1999; Tiral *et al.*, 2006, 2008; Kydonakis *et al.*, 2015).

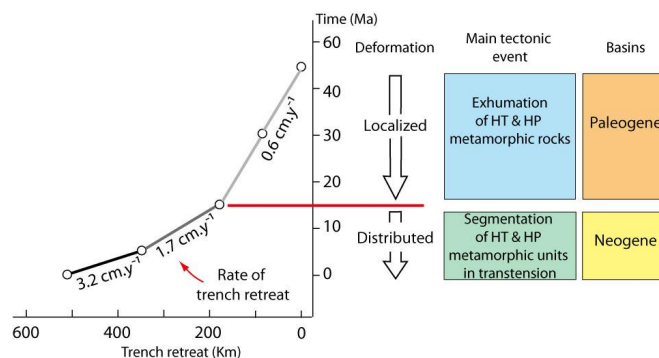


Fig. 5 - Modes of extension as a function of the rate of trench retreat.

The acceleration of trench retreat is more likely related to the Hellenic slab tearing whose rather complex geometry was recently evidenced by S-wave tomography (Salaün *et al.*, 2012). Whereas the exact timing of slab tearing is difficult to constrain, the sudden change in the mode of extension, which is associated with the acceleration of slab retreat, strongly supports that slab tearing should have started to develop earlier, possibly in Early Miocene, to become fully efficient from 15 Ma onward.

The transtensional deformation pattern (Fig. 4) that results from the interaction between Hellenic trench retreat and Anatolia westward displacement and that is still active in the Aegean took place in Middle Miocene, as previously argued by Dewey and Şengör (1979) and Şengör *et al.* (2005). Consequently, *the westward displacement of Anatolia was coeval with the acceleration of trench retreat*. Whereas the North Anatolian Fault plays a major role in the present-day kinematic pattern, *the 450 km-long Myrthes-Ikaria Fault-IBTF (Fig. 4) was the first large dextral strike-slip fault zone*

to develop. Its location close to the Izmir-Ankara suture zone and parallel to it strongly suggests that the suture zone was acting as weak zone able to localize displacements at the onset of Anatolia westward displacement; as illustrated by the laboratory experiments of Philippon *et al.* (2014). However, this interaction between two plate boundary displacements raises a fundamental issue: What is the dynamic relationship between slab tearing and Anatolia displacement? Which one controlled the development of the other?

4. References

- Armijo, R., Meyer, B., Hubert, A. and Barka, A., 1999. Westward propagation of the north Anatolian into the northern Aegean: timing and kinematics, *Geology*, 27, 267-270.
- Brix, M.R., Stöckhert, B., Seidel, E., Theye, T., Thomson, S.N. and Küster, M., 2002. Thermobarometric data from a fossil zircon partial annealing zone in high pressure-low temperature rocks of eastern and central Crete, Greece, *Tectonophysics*, 349, 309-326.
- Brun, J.-P., 1999. Narrow rifts versus wide rifts: Inferences for the mechanics of rifting from laboratory experiments. *Philosophical Transactions of the Royal Society*, London, Ser. A 357, 695-712.
- Brun, J.-P. and Faccenna, C., 2008. Exhumation of high-pressure rocks driven by slab rollback, *Earth and Planetary Science Letters*, 272, 1-7, doi: 10.1016/j.epsl.2008.02.038.
- Brun, J.-P. and Sokoutis, D., 2007. Kinematics of the Southern Rhodope Core Complex (north Greece), *International Journal of Earth Sciences*, 96, 1079-1099.
- Brun, J.-P. and Sokoutis, D., 2010. 45 m.y. of Aegean crust and mantle flow driven by trench retreat, *Geology*, 38, 815-818, doi: 10.1130/G30950.1.
- Brun, J.-P., Tirel, C., Philippon, M., Burov, E., Faccenna, C., Gueydan, F. and Lebedev, S., 2012. On the role of horizontal displacements in the exhumation of high pressure metamorphic rocks, *Geophysical Research Abstracts*, 14, EGU2012-9381.
- Buck, W.R., 1991. Modes of continental lithospheric extension, *Journal of Geophysical Research*, 96(B12), 20161-20178.
- Carras, N. and Georgala, D., 1998. Upper Jurassic to Lower Cretaceous Carbonate Facies of African Affinities in a Peri-European Area: Chalkidiki Peninsula, Greece, *Facies*, 38, 153-164.
- Channell, J.E.T. and Kozur, H., 1997. How many oceans? Meliata, Vardar, and Pindos oceans in Mesozoic Alpine paleogeography, *Geology*, 25, 183-186.
- Dercourt, J., Ricou, L.E. and Vrielynck, B., 1993. Atlas Tethys Paleoenvironmental Maps, Beicip-Franlab, Deschamps, R., Hamon, Y., Darre, T. and Gorini, C., 2013. Caractérisation des séries lacustres du Miocène Supérieur de l'île de Samos. Un exemple de paléolac alcalin et salin, *In: 14eme Congrès Français de Sédimentologie*, Paris (Ed. ASF), 73, 118.
- Dewey, J.F. and Şengör, A.C., 1979. Aegean and surrounding regions: complex multiplate and continuum tectonics in a convergent zone, *Geological Society of America Bulletin*, 90, 84-92.
- Doutsos, T., Koukouvelas, I., Zelilidis, A. and Kontopoulos, N., 1994. Intracontinental wedging and post-orogenic collapse in Mesohellenic trough, *Geologische Rundschau*, 83, 257-275.
- Ersoy, E.Y., Helvacı, C., Uysal, I., Karaoğlu, Ö., Palmer, M.R. and Dindi, F., 2012. Petrogenesis of the Miocene volcanism along the Izmir-Balıkesir Transfer Zone in western Anatolia, Turkey: implications for origin and evolution of potassic volcanism in postcollisional areas, *Journal of Volcanology and Geothermal Research*, 241-242, 21-38.
- Faccenna, C., Jolivet, L., Piromallo, C. and Morelli, A., 2003. Subduction and the depth of convection in the Mediterranean mantle, *Journal of Geophysical Research*, 108(B2), 2099. <http://dx.doi.org/10.1029/2001JB001690>.
- Faccenna, C., Becker, T.W., Auer, L., Billi, A., Boschi, L., Brun, J.-P., Capitanio, F.A., Funicello, F., Horváth, F., Jolivet, L., Piromallo, C., Royden, L., Rossetti, F. and Serpelloni, E., 2014. Mantle dynamics in the Mediterranean, *Review of Geophysics*, doi: 10.1002/2013RG000444.
- Ferrière, J., Reynaud, J.-Y., Pavlopoulos, A., Bonneau, M., Migiros, G., Chanier, F., Proust, J.-N. and Gardin, S., 2004. Geologic evolution and geodynamic controls of the Tertiary intramontane piggyback Meso-Hellenic basin, Greece, *Bulletin de la Société Géologique de*

- France, 175, 361-381.
- Görür, N. and Okay, A.I., 1996. A fore-arc origin for the Thrace Basin, NW Turkey, *Geologische Rundschau*, 85, 662-668.
- Hollenstein, C., Müller, M.D., Geiger, A. and Kahle H.-G., 2008. Crustal motion and deformation in Greece from a decade of GPS measurements, 1993-2003, *Tectonophysics*, 449, 17-40, <http://dx.doi.org/10.1016/j.tecto.2007.12.006>.
- Hubert-Ferrari, A., King, G., Manighetti, I., Armijo, R., Meyer, B. and Tapponnier, P., 2003. Long-term Elasticity in the Continental Lithosphere; Modelling the Aden Ridge Propagation and the Anatolian Extrusion Process, *Geophysical Journal International*, 153, 111-132.
- Jolivet, L. and Brun, J.-P., 2010. Cenozoic geodynamic evolution of the Aegean, *International Journal of Earth Sciences*, 99 (1), 109-138, doi: 10.1007/s00531-008-0366-4.
- Jolivet, L. and Faccenna, C., 2000. Mediterranean extension and the Africa-Eurasia collision, *Tectonics*, 19, 1095-1106.
- Jolivet, L., Trotet, F., Monié, P., Vidal, O., Goffé, B., Labrousse, L., Agard, P. and Ghorbal, B., 2010. Along-strike variations of P-T conditions in accretionary wedges and syn-orogenic extension, the HP-LT Phyllite-Quartzite Nappe in Crete and the Peloponnese, *Tectonophysics*, 480, 133-148, doi: 10.1016/j.tecto.2009.10.002.
- Jolivet, L., Faccenna, C., Huet, B., Labrousse, L., Le Pourhiet, L., Lacombe, O., Lecomte, E., Burov, E., Denèle, Y., Brun, J.-P., Philippon, M., Paul, A., Salaün, G., Karabulut, H., Piromallo, C., Monié, P., Gueydan, F., Okay, A.I., Oberhänsli, R., Pourteau, A., Augier, R., Gadenne, L. and Driussi, O., 2013. Aegean tectonics: Strain localisation, slab tearing and trench retreat, *Tectonophysics*, 597, 1-33, doi: 10.1016/j.tecto.2012.06.011.
- Kilias, A., Falalakis, G., Sfeikos, A., Papadimitriou, E., Vamvaka, A. and Gkarlaoui, C., 2013. The Thrace basin in the Rhodope province of NE Greece - A tertiary supradetachment basin and its geodynamic implications, *Tectonophysics*, 595-596, 90-105.
- Koukouvelas, I.K. and Aydin, A., 2002. Fault structure and related basins of the North Aegean Sea and its surroundings, *Tectonics*, 21, 1046. <http://dx.doi.org/10.1029/2001TC901037>.
- Kydonakis, K., Brun, J.-P. and Sokoutis, D., 2015a. North Aegean core complexes, the gravity spreading of a thrust wedge, *Journal of Geophysical Research*, Solid Earth, 120, doi: 10.1002/2014JB011601.
- Le Pichon, X. and Angelier, J., 1981. The Aegean Sea. *Philos. Philosophical Transactions of the Royal Society*, London, Ser. A 300, 357-372.
- Lyberis, N., 1984. Tectonic evolution of the North Aegean trough, Geological Society, London, Special Publications, 17, 709-725.
- Marsellos, A.E., Min, K. and Foster, D.A., 2014. Rapid Exhumation of High-Pressure Metamorphic Rocks in Kythera-Peloponnese (Greece) Revealed by Apatite (U-Th)/He Thermochronology, *The Journal of Geology*, 122, 381-396.
- Masche, J. and Martin, L., 1990. Shallow structure and recent evolution of the Aegean Sea: A synthesis based on continuous reflection profiles, *Marine Geology*, 94, 271-299. doi: 10.1016/0025-3227(90)90060-W.
- McClusky, S., Balassanian, S., Barka, A., Demir, C., Ergintav, S., Georgiev, I., Gurkan, O., Hamburger, M., Hurst, K., Kahle, H., Kastens, K., Kekelidze, G., King, R., Kotzev, V., Lenk, O., Mahmoud, S., Mishin, A., Nadariya, M., Ouzounis, A., Paradissis, D., Peter, Y., Prilepin, M., Reilinger, R., Sanli, I., Seeger, H., Tealeb, A., Toksöz, M.N. and Veis, G., 2000. Global Positioning System constraints on plate kinematics and dynamics in the eastern Mediterranean and Caucasus, *Journal of Geophysical Research*, Solid Earth, 105, 5695-5719.
- McKenzie, D.P. 1972. Active tectonics of the Mediterranean region. *Geophysical Journal of the Royal Astronomical Society*, 30, 109-185.
- McKenzie, D.P., 1978. Active tectonics of the Alpine Himalayan Belt, the Aegean Sea and surrounding regions. *Geophysical Journal of the Royal Astronomical Society*, 55, 217-252.
- Mercier, J.-L., Sorel, D. and Simeakis, K., 1987. Change in the state of stress in the overriding plate of a subduction zone: the Aegean Arc from the Pliocene to the present, *Annales Tectonicae*, 1, 20-39.

- Mercier, J.-L., Sorel, D., Vergely, P. and Simeakis, K., 1989. Extensional tectonic regimes in the Aegean basins during the Cenozoic, *Basin Research*, 2, 49-71.
- Müller, M.D., Geiger, A., Kahle, H.-G., Veis, G., Billiris, H., Paradissis, D. and Felekis, S., 2013. Velocity and deformation fields in the North Aegean domain, Greece, and implications for fault kinematics, derived from GPS data 1993-2009, *Tectonophysics*, 597-598, 34-49. <http://dx.doi.org/10.1016/j.tecto.2012.08.003>.
- Philippon, M., Brun, J.P. and Gueydan, F., 2012. Deciphering subduction from exhumation in the segmented Cycladic Blueschist Unit (Central Aegean, Greece), *Tectonophysics*, 524, 116-134, doi:10.1016/j.tecto.2011.12.025.
- Philippon, M., Brun, J.-P., Gueydan, F. and Sokoutis, D., 2014. The interaction between Aegean back-arc extension and Anatolia escape since Middle Miocene, *Tectonophysics*, 631, 176-188, doi:10.1016/j.tecto.2014.04.039.
- Piomallo, C. and Morelli, A., 2003. P wave tomography of the mantle under the Alpine-Mediterranean area, *Journal of Geophysical Research*, Solid Earth, 108(B2), 2065.
- Robertson, A., 2004. Development of concepts concerning the genesis and emplacement of Tethyan ophiolites in the Eastern Mediterranean and Oman regions, *Earth-Science Reviews*, 66, 331-387.
- Roussos, N., 1994. Stratigraphy and paleogeographic evolution of Palaeocene molassic basins of N. Aegean, *Bulletin of the Geological Society of Greece*, XXX, 275-294.
- Royden, L.H., 1993. The tectonic expression slab pull at continental convergent boundaries, *Tectonics*, 12, 629-638.
- Sakellariou, D., Mascle, J. and Lykousis, V., 2013. Strike slip tectonics and transtensional deformation in the Aegean region and the Hellenic arc: preliminary results, *Bulletin of the Geological Society of Greece, XLVII, Proceedings of the 13th International Congress*, Chania, Sept. 2013.
- Salaün, G., Pedersen, H., Paul, A., Farra, V., Karabulut, H., Hatzfeld, D., Childs, D.M., Pequegnat, C. and the SIMBAAD Team, 2012. High-resolution surface wave tomography beneath the Aegean-Anatolia region: constraints on upper mantle structure, *Geophysical Journal International*, 190, 406-420, <http://dx.doi.org/10.1111/j.1365-246X.2012.05483.x>.
- Sengör, A.M.C., Tüysüz, O., Imren, C., Sakıncı, M., Eyidogan, H., Görür, N., Le Pichon, X. and Rangin, C., 2005. The North Anatolian Fault: A New Look, *Annual Review of Earth and Planetary Sciences*, 33, 37-112.
- Siyako, M. and Huvaz, O., 2007. Eocene stratigraphic evolution of the Thrace Basin, Turkey, *Sedimentary Geology*, 198, 75-91.
- Sözbilir, H., Sarı, B., Uzel, B., Sümer, Ö. and Akkiraz, S., 2011. Tectonic implications of transtensional supradetachment basin development in an extension-parallel transfer zone: the Kocaçay Basin, western Anatolia, Turkey, *Basin Research*, 23, 423-448, <http://dx.doi.org/10.1111/j.1365-2117.2010.00496.x>.
- Tirel, C., Brun, J.-P. and Sokoutis, D., 2006. Extension of thickened and hot lithospheres: Inferences from laboratory modeling, *Tectonics*, 25, TC1005, doi: 10.1029/2005TC001804.
- Tirel, C., Brun, J.-P., Burov, E., Wortel, M. and Lebedev, S., 2013. A plate tectonics oddity: Caterpillar-walk exhumation of subducted continental crust, *Geology*, 41, 555-558.
- Uzel, B., Sözbilir, H., Özkaymak, C., Kaymakçı, N. and Langereis, C.G., 2013. Structural evidence for strike-slip deformation in the İzmir-Balıkesir transfer zone and consequences for late Cenozoic evolution of western Anatolia (Turkey), *Journal of Geodynamics*, 65, 94-116.
- Widiyantoro, S., van der Hilst, R.D. and Wenzel, F., 2004. Deformation of the Aegean Slab in the Mantle Transition Zone, *International Journal of Tomography and Statistics*, D04, 1-14. December 2004 ISSN 0972-9976.
- Wortel, M.J.R. and Spakman, W., 2000. Subduction and slab detachment in the Mediterranean-Carpathian region, *Science*, 290, 1910-1917.
- Wuthrich, E., 2009. Low temperature thermochronology of the North Aegean Rhodope Massif, Ph.D. thesis, Swiss Federal Institute of Technology, Zurich.

THREE-DIMENSIONAL ANALYSIS OF NORMAL FAULT ZONES IN KARDIA MINE, PTOLEMAIS BASIN, NW GREECE

Delogkos E.¹, Manzocchi T.¹, Childs C.¹, Sachanidis C.², Barmpas T.²,
Chatzipetros A.³, Walsh J.J.¹ and Pavlides S.³

¹Fault Analysis Group, School of Earth Sciences, University College Dublin, Dublin, Ireland,
efstratios.delogkos@ucdconnect.ie, tom.manzocchi@ucd.ie, conrad.childs@ucd.ie,
john.walsh@ucd.ie

²Public Power Corporation of Greece, Western Macedonian Lignite Centre, Ptolemais, Greece,
c.sachanidis@dei.com.gr, tr.barmpas@dei.com.gr

³Aristotle University of Thessaloniki, School of Geology, Thessaloniki, Greece,
pavlides@geo.auth.gr, ac@geo.auth.gr

Abstract

Six normal fault zones, with throws ranging from a few meters up to 50 m, were studied within an active, open pit, lignite mine in Ptolemais. Each fault was mapped 20 times over a period of five years because at intervals of ca. 3 months working faces are taken back between 20 and 50 m exposing fresh fault outcrops for mapping. Various resolutions of photographs and structural measurements were imported into a fully georeferenced 3D structural interpretation package, resulting in aseismic scale and outcrop resolution 3D fault volume with outcrop and panoramic photographs acting as the seismic sections in equivalent seismic surveys. Low resolution 3D models for the fault system structure at mine scale and higher-resolution 3D models for the fault zone structure were produced after geological interpretation and they can be used for qualitative and quantitative analysis.

Keywords: Normal faults, Fault geometry, 3D structural model, Kardias lignite mine.

Περίληψη

Έξι ζώνες κανονικών ρηγμάτων, με μεταπτώσεις που κυμαίνονται από λίγα έως 50 μέτρα, μελετήθηκαν μέσα σε ένα ενεργό, επιφανειακό λιγνιτωρυχείο στην Πτολεμαΐδα. Κάθε ρήγμα χαρτογραφήθηκε 20 φορές σε χρονικό διάστημα πέντε ετών, σε διαστήματα περίπου 3 μηνών, καθώς κάθε πρηνές μετακινείται προς τα πίσω κατά 20 με 50 μέτρα λόγω της εκσκαφής, εκθέτοντας καινούργιες εμφανίσεις ρηγμάτων για χαρτογράφηση. Φωτογραφίες και τεκτονικές μετρήσεις εισήχθησαν σε ένα λογισμικό, με πλήρη γεωαναφορά στο τρισδιάστατο χώρο, με αποτέλεσμα ένα τρισδιάστατο όγκο ρηγμάτων "σεισμικής κλίμακας" αλλά με ανάλυση πεδίου, με τις φωτογραφίες να ενεργούν σαν σεισμικές τομές στις αντίστοιχες σεισμικές έρευνες. Χαμηλότερης ανάλυσης 3D μοντέλα παρήχθησαν μετά την γεωλογική ερμηνεία για την ποιοτική και ποσοτική μελέτη της δομής του συστήματος ρηγμάτων σε κλίμακα ορυχείου και υψηλότερης ανάλυσης 3D μοντέλα, για τη μελέτη της δομής της ρηξιγενούς ζώνης σε κλίμακα πεδίου.

Λέξεις κλειδιά: Κανονικά ρήγματα, Γεωμετρία ρηγμάτων, Τρισδιάστατο μοντέλο, Λιγνιτωρυχείο Καρδιάς.

1. Introduction

Faults are zones of extreme internal complexity and heterogeneous strain distribution over a wide range of scales. Although this complexity does not lend itself to a simple description to which all faults conform, a simplified and generalised description of faults is required to achieve a better understanding of fault evolution and for many practical applications, such as the production of oil from faulted reservoirs and earthquake hazard assessment (Childs *et al.*, 2009).

A common feature of faults on all scales is the frequent presence of segmented fault arrays containing two or more fault segments which can be hard-linked by discrete faults or soft-linked by zones of continuous deformation (Peacock and Sanderson, 1991; Walsh and Watterson, 1989, 1990, 1991; Childs *et al.*, 1995, 1996; Walsh *et al.*, 2003). Fault linkage is a dynamic process that evolves with increased displacement (Peacock and Sanderson, 1994; Childs *et al.*, 1995; Walsh *et al.*, 1999; Kristensen *et al.*, 2008).

In the published literature many attempts have been made to investigate and understand the fault zone structure and evolution by qualitative and quantitative analysis of various fault components such as thickness, length and displacement. Such data in the published literature are mainly derived from outcrop studies (2D), detailed geological-fault maps (2D), digital elevation models combined with satellite images (2D) and seismic interpretations (3D).

Data derived from outcrop studies are characterized by their high resolution but lack of a three-dimensional context, in contrast to seismic data which can be fully 3D but have very low resolution compared to outcrop data (the best quality seismic data is unable to resolve faults with throws less than 5 m).

The goal of this paper is to examine the levels of and controls on geometrical complexity of fault zones by using an exceptional dataset which allows a truly 3D analysis of the fault zones at outcrop resolution on a seismic scale. A few similar attempts for 3D investigation of faults at outcrop resolution have been made in the past (Koestler and Reksten, 1995; Childs *et al.*, 1996; Kristensen *et al.*, 2008).

2. Data and Methodology

2.1. Basic Geology and Structure of Kardia Mine

The dataset used in this study is derived from Kardia mine which is one of the four, active, open pit, lignite fields in Ptolemais Basin, W. Macedonia, Greece (Fig. 1). The Ptolemais Basin is an elongated intramontane lacustrine basin and is part of Florina-Ptolemais-Servia Basin which is a NNW-SSE trending graben system that extends over a distance of 120 km from Bitola in the Former Yugoslav Republic of Macedonia (F.Y.R.O.M.) to the village of Servia, south-east of Ptolemais, Greece (Pavlides, 1985). The depression is filled with a 500-600 m (in a few areas up to about 1000 m) thick succession of sediments which are divided into the lower (Upper Miocene to Lower Pliocene) formation, the Pliocene middle formation and the Quaternary upper formation. The Pliocene middle formation contains the upper and lower lignite seams which alternate with clays, marls, sandy marls and sands (Pavlides, 1985; Koufos and Pavlides, 1988).

The basin is bounded by two fault systems which can be related to two extensional episodes (Pavlides and Mountrakis, 1987; Mercier *et al.*, 1989). The first, Late Miocene episode resulted in the origin of the basin in response to NE-SW extension, which was subsequently subjected to NW-SE extension during the Quaternary, resulting in the NE-SW-striking faults which currently bound a number of sub-basins, including the basins of Florina, Ptolemais and Servia (Pavlides and Mountrakis, 1987, Fig. 1).

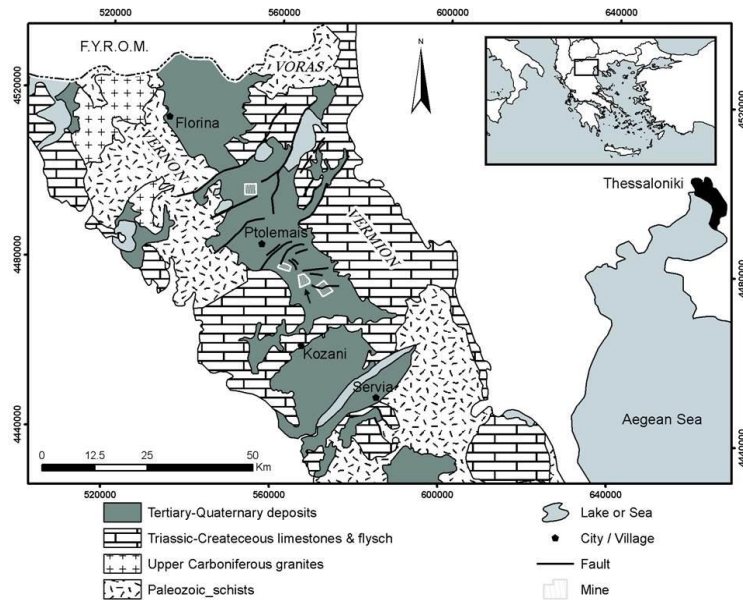


Figure 1 - Simplified geological sketch map of the Florina-Ptolemais-Servia Basin (after Pavlides, 1985; IGME, 1997 and Steenbrink *et al.*, 2000). The black arrow indicates the Kardia lignite field.

Kardia lignite field is situated approximately in the central part of the Neogene lignite basin and is dominated by the later faults which have approximately E-W orientations. In all, six normal fault zones with throws ranging from a few meters up to 50 m displace the lignite-marl sequence in the mine (Fig.2).

The faults form soft-linked systems (Walsh and Watterson, 1991), characterised by a prevalence of fault tips as opposed to branch-points, with ductile bed rotations between faults accommodating transfers of strain between adjacent faults (Fig.3). Quantitative analysis of the faults indicates that these systems are extremely soft and that for a given throw, these faults are both shorter and more segmented than many other fault systems (Fault Analysis Group, 2011; Delogkos, 2011).

2.2. Sampling

As mentioned above, Kardia mine is one of the four active lignite fields in Ptolemais Basin, and every few months fresh fault outcrops are exposed due to the continuous mining operations.

Kardia mine consists of six principal benches and faces which are in average 2.5 km long. The mine faces, with a height of ca. 20 m, step to the west from the bottom to the top of the mine and are separated by the benches which have a width of ca. 100 m (Fig. 4). In each bench, a huge excavator undertakes the excavation of lignite and moves each face back by about 30 m each pass, exhuming fresh outcrop. In addition to the main faces, small faces, with heights up to 4 m, are well exposed in trenches which are created by the excavators in the benches between the main faces (see benches 4 and 5 in Fig. 4).

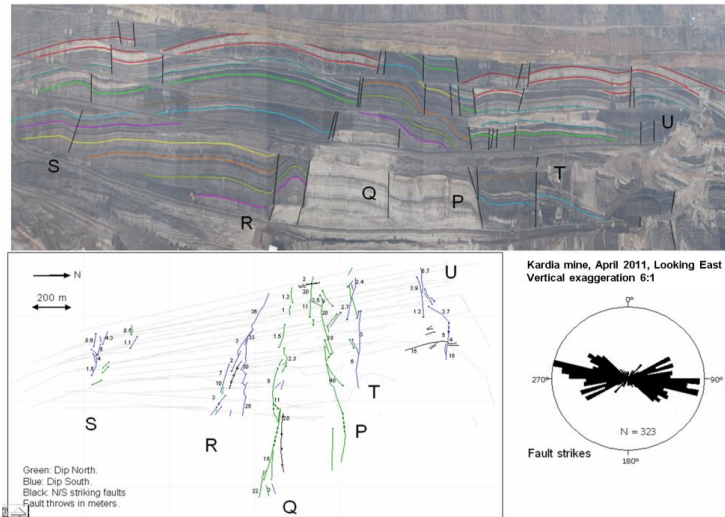


Figure 2 – a) A vertically exaggerated photomontage of the mine showing the faults and some of the horizons, b) a detailed map of the fault zones oriented in sympathy to the photomontage and c) rose diagram summarising the strikes of the normal faults (Fault Analysis Group, 2011).

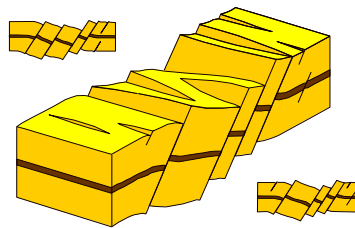


Figure 3 – Cartoon of a soft-linked fault system, characterised by ductile rotation of faults and beds at all stages of deformation (Walsh and Watterson, 1991).

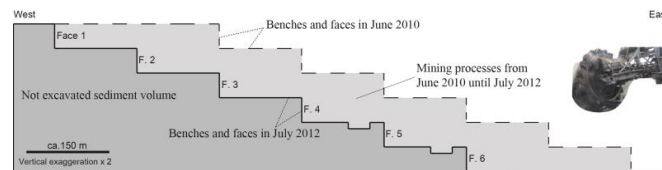


Figure 4 – Cartoon showing a cross-section of Kardia mine. The dashed line shows the faces and the benches as they were in June 2010 and the thick line as they were in July 2012. Light grey colour shows the area that has been excavated from June 2010 to July 2012.

We have visited and mapped the mine 20 times from June 2010 until now, at intervals of ca. 3 months, during which time each face is taken back between 20 and 50 m and fresh fault outcrops are subsequently available for mapping. The data collected during each fieldwork campaign are various resolutions of photographs, accurate GPS locations, structural measurements and interpretations for all the faults and all the other structures observed in the mine, such as normal or

reverse drag. In this paper, the area that is covered by our data is from June 2010 until July 2012, 9 field seasons in total, and it is shown by light grey colour in Fig. 4.

Various resolutions of photographs include: a) A set of panoramic photographs of the whole mine which are taken from a distance of ca. 1.5 km away from the mine faces (Fig. 2.a). b) Outcrop-scale photographs which are taken from a distance of ca. 40 m from each fault, perpendicular to the face and using a meter-stick at the bottom of the face for scale. c) Very high resolution panoramic photographs for individual faults showing in detail the complexity of the fault zones such as multiple fault slip surfaces and lignite or marl smear.

Structural measurements in the field referred to orientations (strike, dip and dip direction) for all main fault slip surfaces, synthetic and antithetic faults. Detailed measurements of orientations were recorded for observable changes in strike and/or dip along the faults at outcrop-scale; abundant vertical strike refraction is a characteristic of these faults. Changes in bedding due to faulting, such as bed rotations within fault zones, normal and reverse drag, were also recorded.

2.3. Workflow for inputting data into a fully georeferenced 3D structural interpretation package

Three-dimensional models of the fault system were produced by placing our data within a fully georeferenced 3D structural interpretation package. For this purpose, TrapTester, a standard oil industry software package for fault analysis is used. This software is designed to input, process and interpret seismic and well data but not photographs of real-world outcrops. Therefore a non-standard import workflow had to be applied.

Given that the XY coordinates for each fault and for the main structures at each individual face in the mine are known, as are the values of absolute altitude at the bottom and top of the mine faces, then the field dataset can be transferred into TrapTester software.

Data covering the whole length of each mining face had to be imported into TrapTester, in order to build mine scale 3D structural model. Each one of the mining faces is cropped from the panoramic photographs and then is imported into TrapTester, in a similar way that the 2D seismic surveys are imported.

In more detail, two main stages must be followed in order to import the cropped pictures, and the higher resolution close-up pictures, into TrapTester. The first stage is to import the 2D navigation lines of a 2D survey, each of which corresponds to a picture, into TrapTester and then the second stage involves definition of the Z-range (“seismic access definition (SIAC)”) for each picture.



Figure 5 – An example of part of a mine face cropped from a panoramic photograph, showing the data required in order to import it into TrapTester. The X_iY_i coordinates and the corresponding pixels of the faults and the left and right end of the picture are needed to create the navigation lines. The X_iY_i coordinates for the left and right end of the picture are not known but they can easily be calculated as the number of pixels per meter is known. The altitude at the bottom of the picture is known and again using the pixels per meter, the altitude at the top can be calculated.

2D navigation lines are in fact the map locations of the cropped pictures, and they are based on the XY coordinates of the faults, left and right ends of each picture and the corresponding horizontal distances in pixels of each picture (Fig. 5). Concerning the SIAC, each one contains information

about Z-shift and Z-scaling which are based on location of the top of the picture with respect to the chosen datum (Z-shift) and number of pixels per vertical meter (Z-scaling).

Structural measurements are imported into TrapTester as tri-mesh surfaces which are displayed in 3D space with the dip and dip-azimuth values as they are measured in the field. The information required for loading these data is XYZ locations and orientation of each structural measurement. These tri-mesh surfaces are a very useful guide for optimizing the precision of the structural interpretations. Additionally they are used to illustrate the complexity of the fault zone structures, such as the strike refraction.

Empty sections can be imported into the 2D survey and they can be used for fault and/or horizon interpretations in areas where there are no available outcrop data but the interpretations are very predictable. Including them in the creation and analysis of the 3D fault volume, makes the final results more realistic and accurate. A particular use of empty sections is for placing faults tips located between two consecutive mapped mining faces.

3. Results

The result of importing our dataset into the 3D structural interpretation package is a volume similar to a 2D seismic survey, a data type common in the oil and gas industry. The difference is that our dataset, while at a seismic scale, has outcrop-scale resolution.

This exceptional dataset is used for fault and horizon interpretations. Each fault zone is characterized by about 60 cross-sections perpendicular to ca. 900 m long and 20 to 80 m high areas of the fault surface (Figs. 6 and 7).

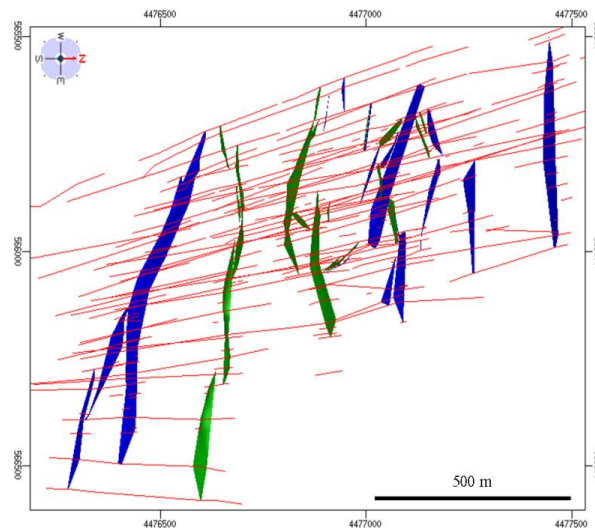


Figure 6 – Map view of the interpreted fault zones from Kardia mine. Interpretations are based on data derived from nine field seasons and cover the area shown by the navigation lines (red lines). South-dipping faults are shown with blue colour and north-dipping faults with green colour.

The layering of lignite and marl makes these sediments ideal for detailed displacement analysis along the faults in cross-section and along strike as individual horizons are continuous across the scale of the structures investigated.

Various resolutions of fault interpretations and respectively 3D models can be made. We use this dataset to build low resolution 3D models for the fault system structure at mine scale (Fig. 7) and higher-resolution 3D models for the fault zone structure (Fig. 8). The fault zone is a part of a fault system.

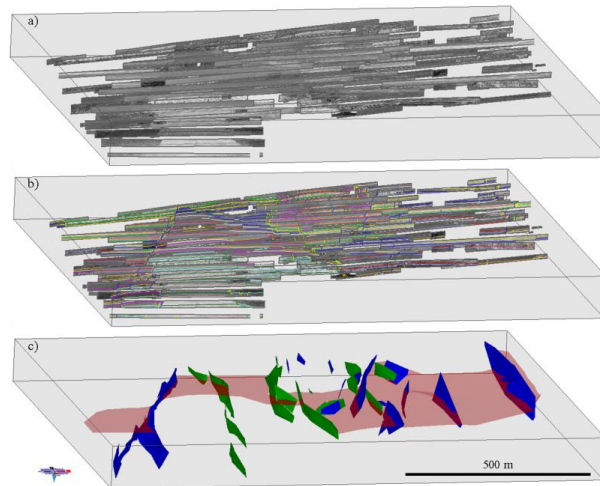


Figure 7 – Lateral view of the 3D TrapTester model showing: a) All the mining faces, which are cropped from the panoramic photographs and are imported into TrapTester like seismic sections. b) As (a) but including fault and horizon interpretations. c) Interpretation of the data showing five fault zones, the majority of which comprise several fault surfaces, which displace the lignite-marl sequence up to 40 meters. The blue fault surfaces dip to the south, and green fault surfaces dip to the north. The transparent red surface, which is displaced by the faults, is one of the interpreted horizons and is located near the middle of the exposed stratigraphic sequence.

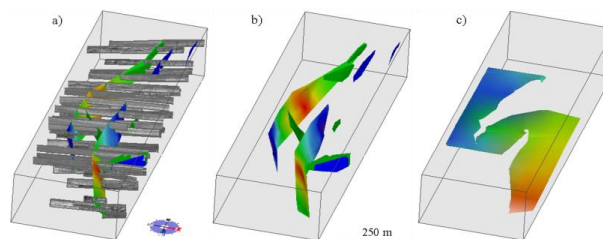


Figure 8 – Lateral view of the 3D TrapTester model showing a fault zone with maximum throw of ca. 36 m. This is actually an almost intact relay zone and consists of two main fault surfaces, a minor breaching fault and some synthetic and antithetic faults. a) All data. b) All the interpreted faults. The variation of the colours on the two main fault surfaces shows the displacement distribution (red is high displacement). The displacement is transferred between the relay bounding faults by bed rotation (c) and small offset along the minor breaching fault. c) One of the interpreted horizons showing the bed rotation within the relay zone. The variation of the colours shows the depth (red in deeper).

In order to build the 3D fault system model, minor synthetic and antithetic faults are ignored and only the main faults and the main structure of the lignite-marl sequence which was displaced and

deformed because of faulting are interpreted. In contrast, for the high resolution 3D fault zone models, all the fault structures are taken into account.

The final 3D fault models can be used for qualitative and quantitative analysis of the fault system and fault zone structure providing insights on the growth, propagation, evolution and geometrical complexity of faults, which will provide a basis for improving conceptual models of fault systems and fault zones, which underpin many practical applications such as the production of oil and gas from faulted reservoirs and earthquake hazard assessment.

4. Conclusions

Using this exceptional dataset from the active opencast lignite field in the Ptolemais basin, we construct 3D fault zone models at outcrop resolution on a seismic scale by importing various resolutions of photographs and structural measurements into a fully georeferenced 3D structural interpretation package. These models allow us to investigate and analyse fault zone structure in 3D, and at outcrop resolution, a combination impossible to accomplish using either outcrop or seismic data.

5. Acknowledgements

This work was carried out as part of the Earth and Natural Sciences Doctoral Studies Programme, funded by the Higher Education Authority (HEA) through the Programme for Research at Third Level Institutions, Cycle 5 (PRTL-5), co-funded by the European Regional Development Fund (ERDF). The work was also funded by the multi-company QUAFF project. The authors would like to thank Badley Geoscience Ltd. for the use of TrapTester6 software. The authors also thank the Public Power Corporation (ΔΕΗ/ΑΚΠΙΑ) for permission to work in the mines and the corporation's employees for their hospitality and assistance in the field during the last four years. Thanks to the other members of the Fault Analysis Group for the field assistance and useful discussions.

6. References

- Childs, C., Watterson, J. and Walsh, J.J., 1995. Fault overlap zones within developing normal fault systems, *Journal of the Geological Society*, London, 152, 535-549.
- Childs, C., Watterson, J. and Walsh, J.J., 1996. A model for the structure and development of fault zones, *Journal of the Geological Society*, 153, 337-340.
- Childs, C., Manzocchi, T., Walsh, J.J., Bonson, C.G., Nikol, A. and Schöpfer, M.P.J., 2009. A geometric model of fault zone and fault rock thickness variations, *Journal of Structural Geology*, 31(2), 117-127.
- Delogkos, E., 2011. Quantitative analysis of geometric evolution of fault zones of Mavropigi lignite field in Ptolemais Basin (W. Macedonia, Greece), Master thesis, Aristotle University of Thessaloniki, Greece, 98 pp.
- Fault Analysis Group, UCD., 2011. Structural geological observations in the Ptolemais lignite mines - a preliminary report, Unpublished.
- Koestler, A.G. and Reksten, K., 1995. Fracture-network 3D characterization in a deformed chalk reservoir analogue - the Lagerdorf case, *SPE Formation Evaluation*, 10(3), 148-152.
- Koufos, G. and Pavlides, S., 1988. Correlation between the continental deposits of the lower Axios valley and Ptolemais basin, *Bull Geol. Soc. Greece*, 20, 9-19.
- Kristensen, M.B., Childs, C.J. and Korstgerd, J.A., 2008. The 3D geometry of small-scale relay zones between normal faults in soft sediments, *Journal of Structural Geology*, 30, 257-272.
- Mercier, J.L., Sorel, D. and Vergely, P., 1989. Extensional tectonic regimes in the Aegean basins during the Cenozoic, *Basin Res.*, 2, 49-71.
- Pavlides, S., 1985. Neotectonic evolution of the Florina-Vegoritiss-Ptolemais basins, PhD thesis, University of Thessaloniki Greece, 256 pp.

- Pavlidis, S.B. and Mountrakis, D.M., 1987. Extensional tectonics of northwestern Macedonia, Greece, since the late Miocene, *J. Struct. Geol.*, 9(4), 385-392.
- Peacock, D.C.P. and Sanderson, D.J., 1991. Displacement and segment linkage and relay ramps in normal fault zones, *Journal of Structural Geology*, 13, 721-733.
- Peacock, D.C.P. and Sanderson, D.J., 1994. Geometry and development of relay ramps in normal fault systems, *American Association of Petroleum Geologists Bulletin*, 78, 147-165.
- Steenbrink, J., Van Vugt, N., Kloosterboer-van Hoeve, M.L. and Hilgen, F.J., 2000. Refinement of the Messinian APTS from sedimentary cycle patterns in the lacustrine Lava section (Servia Basin, NW Greece), *Earth Planet. Sci. Lett.*, 181(3-4), 161-173.
- Walsh, J.J. and Watterson, J., 1989. Displacement gradients on fault surfaces, *Journal of Structural Geology*, 11, 307-316.
- Walsh, J.J. and Watterson, J., 1990. New methods of fault projection for coalmine planning, *Proc. Yorks. Geol. Soc.*, 48, 209-219.
- Walsh, J.J. and Watterson, J., 1991. Geometric and kinematic coherence and scale effects in normal fault systems. In: *Geometry of Normal Faults*, Roberts, A., Yielding, G. and Freeman, B., eds., *Spec. Pubis Geol. Soc. Lond.*, 56, 193-203.
- Walsh, J.J., Watterson, J., Bailey, W. and Childs, C., 1999. Fault relays, bends and branch-lines, *Journal of Structural Geology*, 21, 1019-1026.
- Walsh, J.J., Bailey, W.R., Childs, C., Nicol, A. and Bonson, C.G., 2003. Formation of segmented normal faults: a 3-D perspective, *Journal of Structural Geology*, 25, 1251-1262.